doi:10.1017/S143192762200722X
Microsc. Microanal. 28 (Suppl 1), 2022

2D to 3D Structural Transformation of Calcium Oxalate Revealed by *In Situ* Graphene Liquid Cell TEM

Lioudmila V. Sorokina[1], Abhijit H. Phakatkar[2], Reza Shahbazian-Yassar[1,3], and Tolou Shokuhfar[2,3*]

[1.] Department of Civil, Materials, and Environmental Engineering, University of Illinois at Chicago, Chicago, IL, United States.
[2.] Department of Biomedical Engineering, University of Illinois at Chicago, Chicago, IL, United States.
[3.] Department of Mechanical Engineering, University of Illinois at Chicago, Chicago, IL, United States.
* Corresponding author: tolou@uic.edu

Calcium oxalate, abbreviated CaOx, is a widely occurring biomineral responsible for a variety of essential plant functions such as photosynthesis, regulation of calcium, and structural integrity, to name a few [1, 2]. By contrast, in humans, CaOx is a key constituent in kidney stone formation, a disease that impacts approximately 12% of the worldwide population [3]. Greater than 70% of all kidney stones are composed of calcium oxalate and calcium oxalate mixed with other minerals such as calcium phosphate [4, 5]. This provides great incentive to study the mechanisms of CaOx crystal nucleation and growth, which are still not well understood.

CaOx can form three distinct phases as it crystallizes. From the least stable to the most stable they are: calcium oxalate trihydrate (COT), calcium oxalate dihydrate (COD), and calcium oxalate monohydrate (COM). An amorphous phase was found to be an intermediary in the non-classical crystallization of CaOx in the presence of citrate [6]. From a clinical perspective, COM and COD are phases of interest due to their thermodynamic stability and prevalence in kidney stone specimens. In order to design appropriate solutions, it is therefore important to understand the mechanisms of nucleation and growth as well as any underlying phase transformations in the crystallization of metastable and stable phase of CaOx.

Previously, our group established that COM can form follow either classical or non-classical pathway to crystal formation [7]. Moreover, we determined that the addition of citrate, a known inhibitor, can increase the hydration state of CaOx, thereby making it more unstable. In the present study, we use *in situ* graphene liquid cell (GLC) transmission electron microscopy (TEM) to explore the transformation from two-dimensional to three-dimensional COD and the underlying key events. In order to accomplish this, we encapsulated a supersaturated solution containing calcium and oxalate ions between graphene-coated TEM grids to observe nucleation and growth in metastable CaOx in real time. Data acquisition was performed at 200 keV using a single tilt TEM holder. Key events are presented in Figure 1.

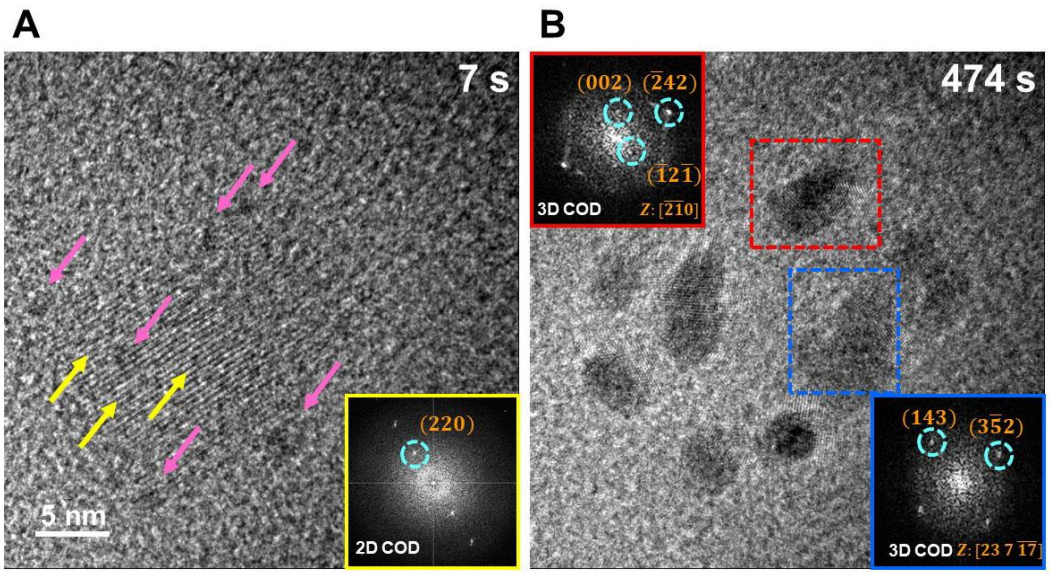

Figure 1. HR-TEM micrographs of calcium oxalate dihydrate (COD) 2D nanosheet transformation into COD 3D nanoparticles. (A) Initial 2D nanosheet structure with corresponding Fast Fourier Transform (FFT) in the insert; yellow arrows indicate 2D nanosheet while pink arrows show the newly forming nuclei of 3D nanoparticles growing along the sheet's periphery (B) 3D nanoparticles coalesce and grow, with final structures identified by FFTs shown in inserts. Scale bar: 5 nm.

Supersaturation, free energy of the solution, and interfacial energy are traditionally thought of factors that, together with the energy from the electron beam, lead to the formation of the initial 2D nanosheet (Figure 1A, yellow arrows). It was previously reported that the unique environment of a graphene liquid cell provides spatial confinement and the graphene acts as a promoter of epitaxial growth [8]. Moreover, the pressure due to encapsulation helps to facilitate in-plane ordering. The FFT of 2D nanosheet confirms COD structure and consists of {110} family of planes, as shown in Figure 1A insert. This suggests that the 2D nanosheet initially forms following the geometry of graphene as this family of planes is also encountered in graphene.The nanosheet continues to disintegrate while simultaneously nucleating 3D nanoparticles along its edges, as shown in Figure 1A by pink arrows. The disintegrating nanosheet acts as a source of localized ions and that of a heterogenous nucleation substrate. 3D particles continue homoepitaxial growth and coalesce, as confirmed by Figure 1B inserts, suggesting non-classical growth in the metastable phase of CaOx.

Coalesence of 3D nanoparticles occurs via oriented attachment, as shown in Figure 2. Specifically, in a multiparticle coalesence event, particles labeled 1,2, and 3 orient themselves along the (141) plane (Figure 2A). All three particles coalesce, and the newly formed single particle also shows the same plane as it continues to grow (Figure 2B). The significance of this work is three-fold. First, we identified the formation of a 2D nanosheet in a graphene liquid cell – a phenomenon likely due to the unique environmental conditions of the latter. Second, we reported for the first time at atomic level resolution, that the 2D to 3D transformation of metastable COD occurs via heterogeneous nucleation. This geometric but not phase transformation suggests a transition aimed to minimize surface energy. This is an important implication since *in vivo* CaOx does not nucleate homogeneously. Lastly, we observed that metastable COD follows a non-classical pathway of nanoparticle growth. To our best knowledge, this is the first reported instance of CaOx nanoparticles coalescing via oriented attachment. This provides knowledge to design therapeutic agents that disrupt attachment along preferred direction of crystal growth [9].

https://doi.org/10.1017/S143192762200722X Published online by Cambridge University Press

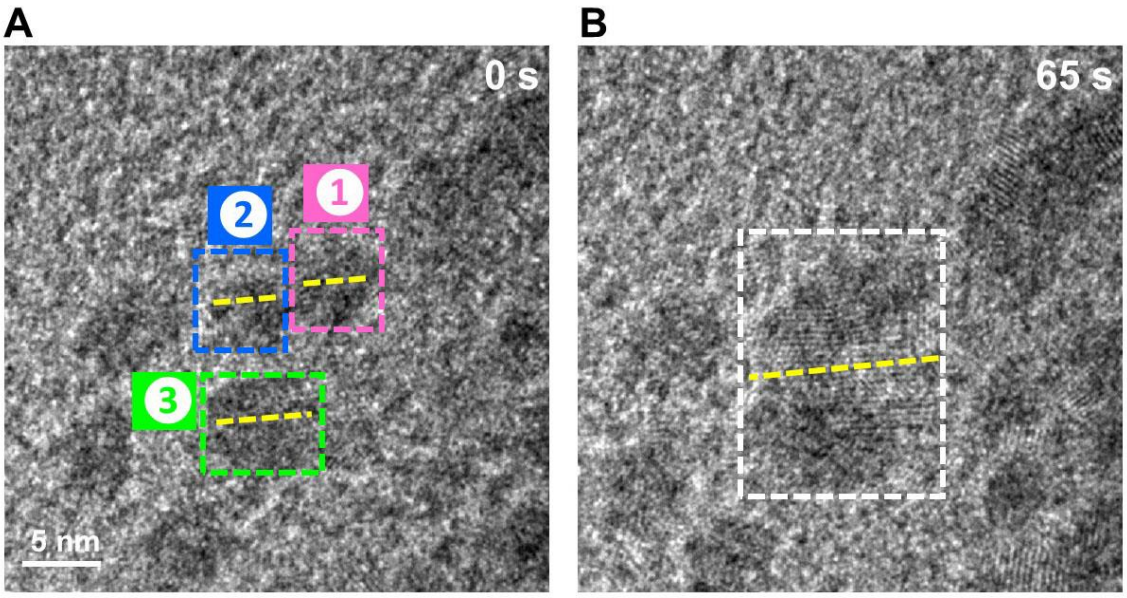

Figure 2. HR-TEM micrographs showing coalescence via oriented attachment in 3D nanoparticles. (A) Particles outlined in pink, blue, and green align themselves along the (141). (B) Post-coalescence newly formed particle becomes denser and continues to grow. Scale bar: 5 nm.

[1] VR Franceschi and PA Nakata, Annu. Rev. Plant Biol. **56** (2005), p. 41.
[2] G Tooulakou et al., Plant Physiology **171** (2016), p. 2577.
[3] T Alelign and B Petros, Advances in urology (2018).
[4] S Lewandowski and AL Rodgers, Clinica Chimica Acta **345** (2004), p. 17.
[5] Z Chen, M Prosperi and VY Bird, Journal of Clinical Urology **12** (2019), p. 296.
[6] E Ruiz-Agudo et al., Nature communications **8** (2017), p. 1.
[7] DJ Banner et al., Advanced Functional Materials **31** (2021), p. 2007736.
[8] S Jiao, C Duan and Z Xu, Scientific reports **7** (2017), p. 1.
[9] T. Shokuhfar acknowledges the financial support from National Science Foundation Award No. DMR-1710049. R. Shahbazian-Yassar is thankful to NSF award DMR-1809439.

https://doi.org/10.1017/S143192762200722X Published online by Cambridge University Press